Many-body calculation of the $2p_{1/2,3/2}$-$2s_{1/2}$ transition energies in Li-like ^{238}U

A. Ynnerman*,† and J. James‡
Physics Department, Clarendon Laboratory, University of Oxford, Oxford OX1 3PU, United Kingdom

I. Lindgren, H. Persson, and S. Salomonson
Department of Physics, Chalmers University of Technology, 412 96 Göteborg, Sweden
(Received 11 March 1994)

We present a relativistic many-body calculation of the $2s_{1/2}$ and $2p_{1/2,3/2}$ ionization energies in Li-like ^{238}U, based on the coupled-cluster singles and doubles approximation with the inclusion of the unretarded Breit interaction, using Dirac-Fock-Breit orbitals. A detailed comparison is made with a similar calculation using ordinary Dirac-Fock orbitals. The calculation yields the transition energies, and by comparison with the recently published experimental values we find the value for the remaining quantum-electrodynamical correction, which is compared with recent Lamb-shift calculations. The importance of an accurate nuclear model for evaluating the nuclear-size effect is also discussed.

PACS number(s): 31.20.Tz, 31.30.Jv, 31.50.+w, 12.20.Ds

I. INTRODUCTION

Accurate calculations on highly charged ions pose several fundamental problems since effects that cannot easily be included in a Hamiltonian formulation of quantum mechanics can no longer be neglected. A full quantum electrodynamical (QED) treatment of the atom is then desired. This is, however, not feasible at present, and the most accurate results will probably be obtained by some combination of the many-body and the QED approaches. The many-body approach, based on perturbation theory or coupled-cluster methods, is known to yield quite accurate results and the remaining QED effect can in most cases be regarded as a small correction. The QED effect is then defined as everything that is left out in the many-body calculation.

The dominating QED effect is for all heavy ions the Lamb shift, which has a leading $\alpha^3 Z^4$ dependence [using hartree atomic units, or $\alpha(\alpha Z)^4$ using relativistic units]. The Feynman diagrams representing the first-order QED effects contributing to the Lamb shift are shown in Fig. 1. These effects are left out in all many-body calculations. In addition, there are a number of effects with leading $(\alpha Z)^3$ dependence. These are mainly due to the virtual electron-positron-pair creation and retardation effects.

For Li-like uranium the energy of the $2s_{1/2}$-$2p_{1/2}$ transition has been measured with high accuracy [1]. Also, several accurate calculations of the Lamb-shift contribution to this transition have recently been performed [2–11]. In order to make comparison with the experimental result it is important to have access to an accurate many-body value. For that reason we have performed such a calculation, based on the coupled-cluster approach with single and double excitations. A similar calculation has been performed by Blundell, Johnson, and Sapirstein [12] and a comparison of the present results shows a small difference due to the inclusion of higher-order terms involving the Breit interaction. It should already here be pointed out that it is a matter of choice whether the effects giving rise to this difference are treated in the many-body procedure or considered as QED corrections.

To match the present experimental accuracy it will also be necessary to evaluate a number of two-photon effects, from bound-state QED, which are left out in the above consideration. These effects will be considered in future works.

The paper is organized as follows. In Sec. II we consider two different single-particle starting points, Dirac-Fock orbitals and Dirac-Fock-Breit orbitals. In Sec. III we investigate the importance of different nuclear charge distributions. Furthermore, in Sec. IV and Sec. V we present the coupled-cluster singles and doubles (CCSD)

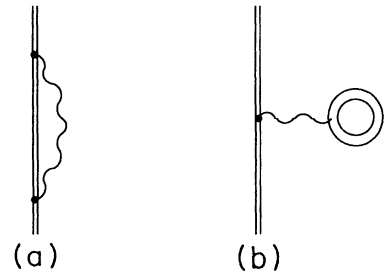

FIG. 1. Feynman diagrams for the lowest-order bound-state self-energy (a) and vacuum polarization (b). Double lines represent propagation in the external potential $V(r)$.

*Electronic address: ynnerman@vuse.vanderbilt.edu
†Present address: Computer Science Department, Vanderbilt University, Nashville, TN 37235.
‡Electronic address: jamesj@vax.ox.ac.uk

calculation. Finally, we give a summary and a future outlook of the field in Sec. VI.

II. SINGLE-PARTICLE ENERGIES

A. Dirac-Fock orbitals

When the special theory of relativity needs to be taken into account, the nonrelativistic Hamiltonian used in the time independent Schrödinger equation is replaced by the Dirac Hamiltonian [13]

$$H = \sum_i^N \left(c\boldsymbol{\alpha} \cdot \mathbf{p} + \beta mc^2 - \frac{Ze^2}{4\pi\epsilon_0 r_i} \right), \tag{1}$$

where c is the speed of light in vacuum and matrices $\boldsymbol{\alpha}$ and β are defined as

$$\boldsymbol{\alpha} = \begin{pmatrix} 0 & \boldsymbol{\sigma} \\ \boldsymbol{\sigma} & 0 \end{pmatrix}, \quad \beta = \begin{pmatrix} I & 0 \\ 0 & -I \end{pmatrix}. \tag{2}$$

Here the $\boldsymbol{\sigma}$ stands for the Pauli spin matrices and I is the two-by-two identity matrix.

A natural extension of the Dirac theory to the many-body case is to define, by analogy with the Hartree-Fock procedure, equations that include the effects of the central part of the field produced by the Coulomb electron-electron interaction, i.e., the central field approximation. This leads to the formulation of the Dirac-Fock (DF) equations. This method has been extensively used for many years, and even multiconfigurational approaches are available [14–16]. The DF procedure provides a good starting point for relativistic many-body calculations.

B. Breit orbitals

When the expression for the electron-electron interaction is derived from QED, the choice of Coulomb gauge has proven to be efficient for bound-state problems. In this gauge the electrons interact through a static Coulomb field and via exchange of virtual transverse photons. In the limit when the energy of the exchanged photon goes to zero, we get the frequency independent interaction potential

$$V(\mathbf{r}_1, \mathbf{r}_2) = \frac{1}{4\pi\epsilon_0} \left(\frac{1}{r_{12}} - \frac{\boldsymbol{\alpha}_1 \cdot \boldsymbol{\alpha}_2}{2r_{12}} - \frac{(\boldsymbol{\alpha}_1 \cdot \mathbf{r}_{12})(\boldsymbol{\alpha}_2 \cdot \mathbf{r}_{12})}{2r_{12}^3} \right), \tag{3}$$

where the second term is half of the unretarded Gaunt interaction, which together with the third term forms the well-known Breit interaction. This expression is correct to order α^2 atomic units [17].

One approach to the inclusion of the Breit interaction, adopted by Blundell, Johnson, and Sapirstein [12], is to use Dirac-Fock orbitals as a starting point for the perturbative expansion. The Breit interaction is then added on as an additional perturbation to lowest order. The diagrams included can be classified as the first-order Breit interaction [Fig. 2(c)], the one-particle diagrams of Breit-RPA (random phase approximation) type [Figs. 3(a,b)], and two-particle diagrams with one Breit interaction [e.g., Fig. 5(b)].

We have adopted an alternative approach. Instead of using the Dirac-Fock Hamiltonian as a basis for the central field approximation, the Breit interaction is added and a new set of one-particle orbitals, Dirac-Fock-Breit (DFB) orbitals, is obtained. Thus the Breit interaction is included self-consistently on the one-particle level. A discussion of the conceptual problems involved in this self-consistent treatment of the Breit interaction has been presented by, e.g., Lindroth *et al.* [18]. On the two-particle level the Breit interaction is treated as a perturbation to first order.

Using DFB orbitals, the effect of all the diagrams shown in Figs. 2, 3, and 4 are included in the orbital energies. Matrix elements between positive-energy DFB orbitals will, in fact, involve both positive- and negative-energy DF orbitals. However, the use of the frequency independent form of the Breit interaction is still justified as long as the Breit interaction occurs only between positive-energy DFB orbitals [18]. In our self-consistent approach we have, apart from all the diagrams of Blundell *et al.* [12], also a number of higher-order diagrams. These are the diagrams including two Breit interactions in Fig. 4, and certain effects of negative-energy DF states, as mentioned above. The size of these effects will be discussed in Sec. V.

III. NUCLEAR CHARGE DISTRIBUTIONS

In a heavy and highly ionized system such as Li-like uranium it is expected that the extension of the nucleus will have a significant influence on the orbital energies, and consideration must be given as to which nuclear potential to use. In a paper by Zumbro *et al.* [19] nuclear parameters for the isotopes ^{233}U, ^{234}U, ^{235}U, and ^{238}U were obtained from muonic x-ray experiments. In the analysis of the muonic data the deformation of the nuclei was taken into account by the introduction of a deformed Fermi distribution, which contains an explicit dependence on the angular coordinates.

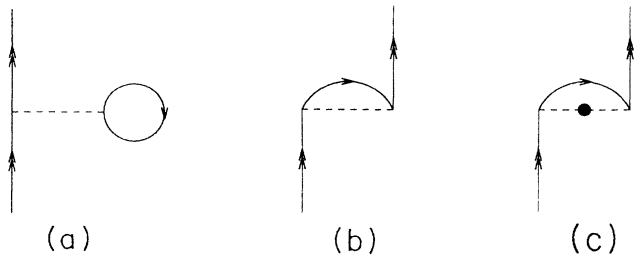

FIG. 2. Goldstone diagrams for the first-order Dirac-Fock, (a) and (b), and Dirac-Fock-Breit (c) contributions to the ionization energy. The dashed line represents the Coulomb interaction and the dashed line with the dot the Breit interaction.

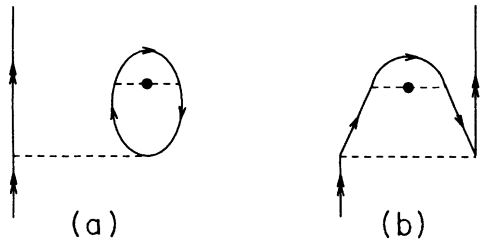

FIG. 3. The second-order contributions to the Breit-RPA chain. This type of diagram is included implicitly in the DFB scheme adopted in this work. The diagrams in which the down-going line represents negative orbitals are included in a self-consistent procedure, but not in a Breit-RPA approach.

$$\rho_{\rm mod}(\mathbf{r}) = \frac{\rho_0}{1+e^{(r-R)/a}}, \tag{4}$$

$$R = c\left[1+\beta_2 Y_{20}(\mathbf{r})+\beta_4 Y_{40}(\mathbf{r})\right]. \tag{5}$$

The relevant values for the parameters for the different isotopes are given in Table I. In the limit where the β coefficients go to zero the ordinary Fermi distribution

$$\rho_{\rm Fermi}(\mathbf{r}) = \frac{\rho_0}{1+e^{(r-c)/a}} \tag{6}$$

is restored.

For a given distribution $\rho(\mathbf{r})$, the spherically averaged potential is given by

$$\Phi(r') = \int_0^r \rho(\mathbf{r}')\frac{r'^2}{r}dr'd\Omega' + \int_r^\infty \rho(\mathbf{r}')\,r'dr'd\Omega'. \tag{7}$$

In the case of the original Fermi distribution [Eq. (6)], following the procedure adopted in the general atomic structure package of computer programs GRASP2 [15,16], the angular dependence can be integrated out and the radial integrals can be written in terms of infinite series, that when evaluated numerically converge to machine precision with just a few terms included. Let

$$\begin{aligned} S_2(x) &= \sum_{n=1}^{\infty} -1^n \frac{e^{xn}}{n^2}, \\ S_3(x) &= \sum_{n=1}^{\infty} -1^n \frac{e^{xn}}{n^3}. \end{aligned} \tag{8}$$

It can then be shown that the potential for $r < c$ can be written as

$$\Phi(r) = \frac{N}{r}\left[\frac{3r}{2c} - \frac{r^3}{2c^3} + \frac{r\pi^2a^2}{2c^3} - \frac{3ra^2}{c^3}S_2\left(\frac{r-c}{a}\right) + \frac{6a^3}{c^3}S_3\left(\frac{r-c}{a}\right) - \frac{6a^3}{c^3}S_3\left(-\frac{c}{a}\right)\right] \tag{9}$$

and for the case when $r > c$ we have

$$\Phi(r) = \frac{N}{r}\left[1 - \frac{6a^3}{c^3}S_3\left(-\frac{c}{a}\right) + \frac{\pi^2a^2}{c^2} + \frac{3ra^2}{c^3}S_2\left(-\frac{r-c}{a}\right) + \frac{6a^3}{c^3}S_3\left(-\frac{r-c}{a}\right)\right]. \tag{10}$$

In these equations N is given by

$$N = \frac{Z}{\left[1 - \frac{6a^3}{c^3}S_3\left(-\frac{c}{a}\right) + \frac{\pi^2a^2}{c^2}\right]}, \tag{11}$$

which follows from the fact that the potential goes to Z/r as r goes to infinity. These expressions for the Fermi distribution can also be used to evaluate the radial parts of the modified distribution for a fixed angle, giving a fixed value of R and thereby an effective c parameter for each angle. Numerical integration over the angular coordinates, using, for instance, Gaussian quadrature then gives the spherically averaged potential originating from the deformed nucleus.

In order to test the importance of the nuclear-size effects we generated Dirac-Fock orbitals using GRASP2 [15,16]. The valence orbitals were generated in the frozen core Dirac-Fock potential of the two $1s$ electrons. A grid with 950 radial points ranging from 0 to 10 bohrs was used. The results for the different isotopes and different nuclear charge distributions were compared to the ionization Dirac-Fock energy for the uranium point nucleus. The results of these calculations are given in Table II. The effect was found to be of the order of 1.3 a.u. for all isotopes when the experimental deformation parameters were used. The values of the parameters were then varied according to the error estimates given in Table I to obtain the errors given. For all the isotopes the errors were found to be of the order of 0.001 a.u. Considering that the error estimates of the deformation parameters are given as "model dependent errors only" [19], this must be regarded as a lower bound to the error induced by the uncertainty of the nuclear parameters. The value obtained for the ^{238}U isotope agrees with the result given in Ref. [12]. Our error estimates are, however, significantly larger.

To estimate the importance of the inclusion of the de-

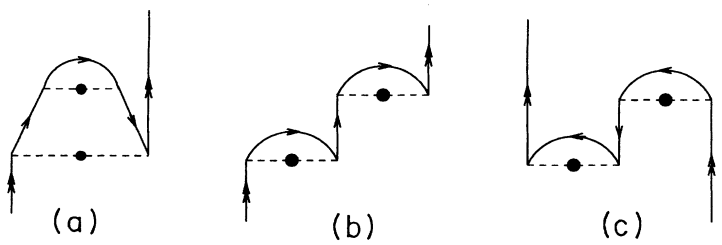

FIG. 4. Second-order diagrams containing two Breit interactions. In (a) and (c) the down-going line can represent both the $1s$ core orbital and the orbitals in the negative-energy continuum.

TABLE I. The nuclear deformation parameters for a modified Fermi distribution, Eqs. (4) and (5) for the different uranium nuclei [19].

Parameter \ Isotope	^{233}U	^{234}U	^{235}U	^{238}U
c (fm)	6.9518(16)	6.9703(13)	6.9858(17)	7.0110(12)
a (fm)	0.5125(12)	0.5089(10)	0.5029(13)	0.5046(9)
β_2	0.2431(40)	0.2507(18)	0.2485(13)	0.2653(14)
β_4	0.091 (15)	0.0843(71)	0.0913(45)	0.0672(49)
$\langle r^2\rangle^{1/2}$ (fm)	5.8158(66)	5.8289(31)	5.8343(28)	5.8604(23)

TABLE II. The nuclear-size contributions to the ground-state energies, in a.u., of the uranium isotopes using a deformed Fermi nucleus, a fitted Fermi nucleus, a uniform distribution, and the default Fermi nucleus, respectively. In the fitted Fermi and the uniform nucleus calculations the rms radius values listed in Table III were used.

Isotope	Deformed Fermi	Fitted Fermi	Uniform	Default Fermi
^{233}U	1.301 80(136)	1.301 53(126)	1.304 95	1.269 44
^{234}U	1.306 07(77)	1.305 81(80)	1.309 23	1.271 82
^{235}U	1.307 87(74)	1.307 61(77)	1.310 99	1.274 21
^{238}U	1.316 40(66)	1.316 09(81)	1.319 53	1.281 32

TABLE III. Parameters for a fitted Fermi distribution using the deformation parameters in Table I, keeping the value of the rms radius fixed.

Parameter \ Isotope	^{233}U	^{234}U	^{235}U	^{238}U
c (fm)	6.9347(18)	6.9526(15)	6.9671(20)	6.9919(15)
a (fm)	0.5997(8)	0.5999(8)	0.5964(10)	0.6023(7)
$\langle r^2\rangle^{1/2}$ (fm)	5.8158(66)	5.8289(31)	5.8343(28)	5.8604(23)

TABLE IV. The nuclear-size contributions to the ground-state ionization energies, in a.u., from a Fermi distribution for ^{238}U using varied values of the rms radius and the skin thickness parameter.

rms radius (fm) \ a	1.2	0.9	0.6023	0.3
5.8550	1.301 28	1.309 52	1.314 32	1.316 94
5.8575	1.302 10	1.310 34	1.315 14	1.317 76
5.8600	1.302 93	1.311 16	1.315 96	1.318 58
5.8625	1.303 76	1.311 98	1.316 78	1.319 40
5.8650	1.304 58	1.312 80	1.317 60	1.320 22

TABLE V. The contributions to the ionization energies, in a.u., of the $2s_{1/2}$ and $2p_{1/2,3/2}$ states in Li-like ^{238}U. FOBR is the retardation effect on the first-order Breit interaction.

Contribution	$2s_{1/2}$	$2p_{1/2}$	$2p_{3/2}$
DFB eigenvalue	−1208.456 70	−1196.572 33	−1042.878 43
Dirac-Fock point	−1211.028 91	−1199.305 71	−1043.786 26
Nuclear size	1.316 40(66)	0.128 83(7)	−0.008 23(5)
FOB	1.263 82	2.628 51	0.926 09
HOB	−0.008 01	−0.023 96	−0.010 03
FOBR	0.023 94	0.010 42	−0.235 35
CCSD	−0.018 41	−0.044 03	−0.015 88
CCSD-Coulomb	−0.010 73	−0.030 77	−0.012 29
Breit-orb in CCSD	−0.000 01	0.000 11	−0.000 01
Coulomb-Breit	−0.007 67	−0.013 37	−0.003 58
Reduced mass	0.002 79	0.002 76	0.002 40
Total	−1208.448 38(66)	−1196.603 18(7)	−1043.127 26(5)

formation the distributions obtained with the parameters in Table I were fitted to a Fermi distribution, Eq. (6), allowing the c and a parameters to float freely, but keeping the root-mean-square (rms) value constant. The results of this fitting are shown in Table III. In the literature [20] the rms value 5.8625 fm for ^{238}U has been used. This value seems to be in error since we have been able to reproduce the rms values for all the isotopes except ^{238}U, for which we find 5.8604 fm. When using the fitted Fermi distributions in Table III the values for the energy were shifted by less than 0.0005 a.u. compared to the deformed Fermi distribution (see Table II).

In Table IV the rms and the skin thickness parameter, for ^{238}U, from the deformed distribution were varied to investigate the sensitivity of the size corrections. The deviation is significant already when small variations are introduced. The importance of the use of accurate nuclear parameters can also be seen by using the default Fermi distribution given in GRASP2 [15,16] as

$$\begin{aligned} \langle r^2\rangle^{1/2} &= 0.836M_{\mathrm{nuc}}^{1/3} + 0.570, \\ a &= \frac{2.30}{4\ln 3}, \\ \langle r^2\rangle &= \frac{3}{5}c^2 + \frac{7}{5}\pi^2 a^2 \end{aligned} \tag{12}$$

for comparison. Here the mass of the nucleus is used to give the values of c and a for a Fermi distribution. To further investigate the model dependence of the nuclear-size corrections the rms value obtained in the fitting procedure was used in a uniform distribution, i.e., in the limit $a \to 0$. The result was a shift in the third decimal place of the energy.

The conclusion is thus that the error introduced by fitting the deformed distribution to a Fermi distribution introduces errors that are somewhat smaller than the errors originating from the uncertainties in the experimental deformation parameters. It is also clear that a relatively crude model, such as the uniform distribution, gives only small errors in the third decimal place as long as the rms value is kept constant. This behavior was noted in a recent paper by Franosch and Soff [21] for the hydrogenlike system. It is, however, essential to have detailed knowledge of the nuclear distribution to obtain a credible value of the rms. As a striking example of this feature the default distribution derived from the mass of the nucleus, Eq. (12), is, as can be seen in Table II, clearly inadequate and introduces errors in the first decimal place of the ionization energy.

IV. CCSD CALCULATION

To evaluate the effect of the electron-electron interaction given in Eq. (3), the CCSD scheme was employed. The exact wave function is written in terms of a zeroth-order wave function, taken to be the Slater determinant of single-particle orbitals, and a wave operator written in the $\exp(S)$ form

$$|\Psi\rangle = \{\exp(S)\}\,|\Psi^0\rangle, \tag{13}$$

where the curly brackets denote normal ordering and S is the cluster operator, which can be divided into one-,. . . ,n-particle excitations

$$S = S_1 + S_2 + \cdots + S_n. \tag{14}$$

The exponential ansatz in combination with the Schrödinger equation leads to a set of coupled equations for the cluster operators. In the CCSD approach only the cluster operators representing one- and two-particle effects are considered. The code that was used for the CCSD calculation is based on a series of previous works [22,23]. The version used in this work is described by Salomonson and Öster [24,25].

Solving the CCSD equations yields the effects of the Coulomb interaction to all orders. This can be represented by diagrams with intermediate states having one or two particles excited. In addition, effects from one Breit and an arbitrary number of Coulomb interactions are included in this work. The no-virtual-pair approximation (NVPA) is employed, i.e., the intermediate states are limited to the positive-energy range.

V. NUMERICAL RESULTS OF CCSD CALCULATION

First, the CCSD calculation was done with DFB orbitals as a starting point. The calculation was performed using a radial grid with 121 points ranging from $\exp(-8)/Z$ to $\exp(4)/Z$. The Coulomb and Breit interactions were expanded in terms of partial waves, which were limited to terms of rank 6 or lower. The numerical results are presented in Table V. In the first line we have the DFB orbital eigenvalues when using a deformed nuclear Fermi distribution with nuclear parameters of Zumbro *et al.* The retardation effect on the first-order Breit interaction was evaluated separately and is presented in line 6 (FOBR). Together with the CCSD contribution and the reduced mass effect we obtain the total energies.

In order to do a detailed comparison with the work of Blundell *et al.* [12] we have analyzed our DFB calculation in terms of a CCSD calculation based on DF orbitals. Thus in Table V we have separated the DFB eigenvalue into the DF eigenvalue and modifications of this eigenvalue from the first-order Breit (FOB) and the remaining part that is due to higher-order effects involving at least one Breit interaction (HOB). The latter part includes diagrams of the type shown in Figs. 3 and 4. All these diagrams are written using a DF basis. It should be noted that it is in this higher-order contribution that the only significant difference between the present calculation and the one performed by Blundell *et al.* is found, and by comparing our HOB numbers with the Breit-RPA numbers by Blundell *et al.* one can note this small but significant discrepancy. In fact, the main difference of the calculated level energies between the two approaches originates from the difference in these values. The discrepancy is partly due to the higher orders of the Breit interaction included in the DFB orbitals and partly due to the effect on these from the negative-energy DF or-

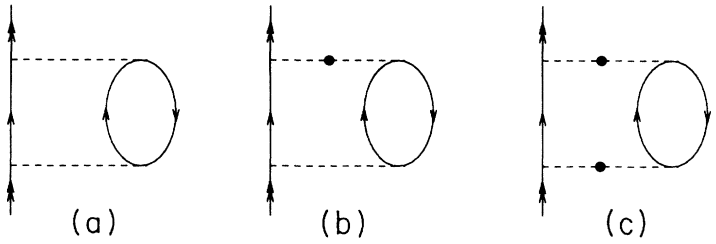

FIG. 5. Second-order diagrams involving the combination of the Coulomb interaction and the Breit interaction. In the actual calculation the Coulomb interaction was represented by the two-particle cluster operator S_2 and the diagram in (c) was neglected.

bitals. In Fig. 4 some additional diagrams involving two Breit interactions, that are included by using DFB orbitals, are shown. In the diagrams in Figs. 3 and 4(a,c) the down-going line represents both the negative-energy continuum and the $1s$ core orbital. In a previous calculation of atomic g_j factors, see Lindroth and Ynnerman [27], this type of negative-energy contributions was found to be very important as well. In Table VI a summary of the contributions from these higher-order Breit diagrams is shown.

As can be seen in Table VI the sum of these second-order effects is quite close to our HOB value. Only the core contributions to the diagrams in Fig. 3, i.e., the first line in Table VI, are included in the calculation by Blundell *et al.* These values are also quite close to their Breit-RPA values. The small differences in both these comparisons are due to effects beyond second order.

We have also separated the CCSD calculation into three different contributions which are given in Table V: First, a pure Coulomb part [e.g., Fig. 5(a) and corresponding higher-order Coulomb diagrams]; second, the effect of using DFB orbitals when evaluating the above diagrams ("Breit-orb in CCSD") which gives very small contributions; and finally, a Breit-Coulomb part [e.g., Fig. 5(b) and corresponding higher-order diagrams in the Coulomb interaction]. These diagrams enter in relative order $Z^2\alpha^2$. Note that the contribution from this effect, given in Table V, is of the same order of magnitude as the second-order Coulomb contribution.

Given that we have calculated an accurate relativistic many-body perturbation theory (RMBPT) value, and taken the nuclear recoil and polarization into account, we can assign the difference between the calculated and the measured transition energy to the pure QED effects. In Table VII the calculated transition energies for $2p_{1/2,3/2}$-$2s_{1/2}$ are given with error estimates.

A comparison with the experimental value [1] gives a value of -41.84(25) eV. The major contribution to the error in this number comes from the uncertainty in the experimental value, 280.59(10) eV and the estimates of the nuclear recoil, -0.08(8) eV, Ref. [6], and nuclear polarization, 0.18(5) eV, Ref. [26]. The Lamb-shift calculation by Persson *et al.* [10,11] lies, as can be seen in Table VII, well within the error limits. However, there are certain two-photon effects which are left out in that calculation. These effects are discussed below in the summary. Also the calculation by Blundell [6], based on methods developed by Snyderman and Blundell [4,5], is within the error limits.

VI. SUMMARY AND OUTLOOK

An accurate RMBPT calculation of the ionization energies of the $2s_{1/2}$ and $2p_{1/2,3/2}$ states in Li-like uranium has been performed. The nuclear-size corrections are calculated using the potential from a deformed nuclear Fermi distribution, with parameters obtained in muonic experiments. For the highly ionized uranium isotopes the inclusion of the Breit interaction in the RMBPT scheme is of great importance both on the one- and the two-particle level.

TABLE VI. The higher-order contribution from the frequency independent Breit interaction. The entries correspond to the diagrams in Figs. 3 and 4. The contributions have been split up into two parts for each diagram containing internal down-going lines, one for the case when the line represents the core orbital and one when the negative-energy orbitals are included. Entries are given in units of 10^{-3} a.u. The total sum compares with the HOB entry in Table V.

Diagram	$2s_{1/2}$	$2p_{1/2}$	$2p_{3/2}$
Figs. 3(a,b) core	−5.775	−18.774	−8.981
Figs. 3(a,b) neg	−0.612	−0.193	−0.201
Fig. 4(a) core	−2.737	−0.470	0.304
Fig. 4(a) neg	0.220	−0.898	0.838
Fig. 4(b)	−2.940	−9.571	−2.004
Fig. 4(c) core	3.637	0.0	0.0
Fig. 4(c) neg	0.195	5.845	0.004
Total	−8.012	−24.061	−10.040
HOB (This work)	−8.01	−23.96	−10.03
Breit-RPA (Blundell *et al.* [a])	−5.91	−18.83	−9.01

[a]Reference [12].

TABLE VII. The contributions to the $2p_{1/2,3/2}$-$2s_{1/2}$, transitions in Li-like U^{238} in eV.

Contribution	$2p_{1/2}$-$2s_{1/2}$	$2p_{3/2}$-$2s_{1/2}$
RMBPT [6,12]	322.324(20)	4498.618
Nuclear recoil[a]	−0.08(8)	−0.04(4)
Nuclear polarization [29]	0.18(5)	0.20(5)
Total	322.43(10)	4498.78(7)
Experiment [1]	280.59(10)	
Difference	−41.84	
QED Persson *et al.* [32]	−41.924	
QED Blundell [6]	−41.68	

[a]Based on $\mathbf{p} = -i\nabla$ and $\mathbf{p} = c\alpha$ for the momentum operator for the two initial states $2p_{1/2,3/2}$, respectively.

Using the accurate experimental value for the $2s_{1/2}$-$2p_{1/2}$ transition a value for the QED effects is extracted and compared with recent Lamb-shift calculations [2–11]. These calculations explain essentially all of the QED shift of the transistion energy. In addition to the first-order self-energy and vacuum polarization, a subset of higher-order QED terms such as the screened self-energy, the screened vacuum polarization, and the combined self-energy vacuum polarization provides a good approximation of the QED shift. Nevertheless, it should be emphasized that to achieve a reliable theoretical value with an uncertainty comparable to the experimental one would require a complete *ab initio* evaluation of all two-photon QED effects. The two-photon effects we have not taken into account in Li-like uranium can be classified into three important categories.

(i) First, there is a part of the two-photon exchange between the electrons, crossed and uncrossed, which is not included in the RMBPT calculation. These effects will be of the same order of magnitude as the higher-order Breit interaction contributions that were evaluated in the present work. Whether these higher-order Breit interactions should be included in the RMBPT calculation or in a QED treatment is a matter of definition.

(ii) Second, there are some second-order self-energy contributions which are expected to be significant at this level of accuracy.

(iii) Finally, the electron screening of the Lamb shift is included only approximately in our earlier calculation procedure.

All these effects are now possible to calculate and will be considered in future works.

In addition, the comparatively low accuracy of the nuclear recoil and polarization estimates limits the extraction of the QED value and an improvement of these values is desirable.

ACKNOWLEDGMENTS

The authors wish to thank Harry Quiney for useful collaborations and stimulating discussions. Eva Lindroth is acknowledged for pioneering the work on the inclusion of the Breit interaction in the CCSD code. Ann-Marie Pendrill has participated in fruitful discussions concerning the Breit-RPA contributions, and Walter Johnson gave a valuable confirmation of the DFB energies. Part of this work was produced at the INT, University of Washington. Financial support was provided by the Swedish and British Royal Societies, the Swedish Institute, the Science and Engineering Research Council (SERC), the Swedish Institute (SI), and the Swedish Natural Research Council (NFR).

[1] J. Schweppe *et al.*, Phys. Rev. Lett. **66**, 1434 (1991).
[2] P. Indelicato and P. J. Mohr, Theor. Chem. Acta **80**, 207 (1991).
[3] K. T. Cheng, W. R. Johnson, and J. Sapirstein, Phys. Rev. Lett. **66**, 2960 (1991).
[4] N. J. Snyderman, Ann. Phys. (N.Y.) **211**, 43 (1991).
[5] S. A. Blundell and N. J. Snyderman, Phys. Rev. A **44**, 1427 (1991).
[6] S. Blundell, Phys. Rev. A **46**, 3762 (1992).
[7] S. Blundell, Phys. Rev. A **47**, 1790 (1993).
[8] K. T. Cheng, W. R. Johnson, and J. Sapirstein, Phys. Rev. A **47**, 1817 (1993).
[9] H. M. Quiney and I. P. Grant, Phys. Scr. **T46**, 132 (1993).
[10] H. Persson, I. Lindgren, and S. Salomonson, Phys. Scr. **T46**, 125 (1993).
[11] I. Lindgren, H. Persson, S. Salomonson, and A. Ynnerman, Phys. Rev. A **47**, 4555 (1993).
[12] S. A. Blundell, W. R. Johnson, and J. Sapirstein, Phys. Rev. A **41**, 1698 (1990).
[13] P. A. M. Dirac, Proc. R. Soc. London, Ser. A **117**, 610 (1928).
[14] I. P. Grant *et al.*, Comput. Phys. Commun. **21**, 207 (1980).
[15] K. G. Dyall *et al.*, Comput. Phys. Commun. **55**, 425 (1989).
[16] F. A. Parpia and I. P. Grant, J. Phys. (Paris) Colloq. **1**, C1-33 (1991).
[17] I. Lindgren, J. Phys. B **23**, 1085 (1990).
[18] E. Lindroth, A.-M. Mårtensson-Pendrill, A. Ynnerman,

and P. Öster, J. Phys. B **22**, 2447 (1989).
[19] J. D. Zumbro *et al.*, Phys. Rev. Lett. **53**, 1888 (1984).
[20] P. Indelicato and E. Lindroth, Phys. Rev. A **46**, 2426 (1992).
[21] T. Franosch and G. Soff, Z. Phys. D **18**, 219 (1991).
[22] I. Lindgren, Int. J. Quantum Chem. **S12**, 33 (1978).
[23] A.-M. Mårtensson, J. Phys. B **12**, 3995 (1979).
[24] S. Salomonson and P. Öster, Phys. Rev. A **40**, 5548 (1989).
[25] S. Salomonson and P. Öster, Phys. Rev. A **41**, 4670 (1990).
[26] G. Plunien, B. Müller, W. Greiner, and G. Soff, Phys. Rev. A **43**, 5853 (1991).
[27] E. Lindroth and A. Ynnerman, Phys. Rev. A **47**, 961 (1993).
[28] H. Persson, I. Lindgren, S. Salomonson, and P. Sunnergren, Phys. Rev. A **48**, 2772 (1993).